Successive linear approximation for large deformations – Instability of salt migration

I-Shih Liu[1*], Rolci A. Cipolatti[1],
Mauro A. Rincon[1], Luiz A. Palermo[2]

[1]Instituto de Matemática, Universidade Federal
do Rio de Janeiro, Brasil
[2]CENPES/Petrobras, Rio de Janeiro, Brasil

Abstract

In continuum mechanics, concerning the motion of a body, besides the Lagrangian and the Eulerian descriptions, the description relative to the present configuration of the body instead of the fixed reference configuration has been known as the relative motion description. Although the relative motion description is mostly ignored in the formulation of boundary value problems, it is interesting to consider such a formulation for the problem in general for solid bodies. In doing so, there is an advantage that when the time increment from the present state is small enough, the nonlinear constitutive equation can be linearized relative to the present configuration, so that the resulting boundary value problem becomes linear.

We can then propose a linear algorithm for large deformation, by building up successive small incremental deformation problem at every time step in the deformation process. In fact, the proposed method is a process of repeated applications of the well-known "small deformation superposed on finte deformation" in the literature.

As an application of the proposed numerical method, we consider instability of a two-layered solid body of a denser material on top of a lighter one. This problem is widely known to geoscientist in sediment-salt migration as salt diapirism. In the literature, this problem has often been treated as Rayleigh–Taylor instability in viscous fluids instead of solid bodies. As an example, we propose a viscoelastic solid material model from constitutive theories of continuum mechanics, and present results of numerical simulations of sediment-salt migration which exhibit main characteristics of salt diapirism as observed by geophysicists.

Keywords: Large deformation, viscoelastic solids, small on large, successive linear approximation, boundary value problem, incremental method, numerical simulation.

Mathematics Subject Classification: 34B15, 74B15, 74D10, 74G15, 74L05.

1 Introduction

The behavior for large deformation is characterized by some genuinely nonlinear constitutive relations, which leads to a system of nonlinear partial differential equations. To solve boundary value problems of this nonlinear system for large deformation with finite elements, variational forms are usually formulated in Lagrangian or Eulerian domains, which result in nonlinear discrete equations.

*Corresponding author: I-Shih Liu, e-mail: liu@im.ufrj.br

For large deformations in solids, many problems cannot be treated effectively with Lagrangian meshes in the fixed reference domain, nor with Eulerian meshes in the spatial domain of the body. Therefore the hybrid technique of arbitrary Lagrangian Eulerian formulation (ALE) has been developed (see for example [1]), in which an arbitrary judicious choice of mesh motion is selected as an intermediate reference state to minimize the mesh distortion. In other words, the state from an arbitrary mesh motion is chosen as the reference state for the problem.

Theoretically, any state can be chosen as a reference state, and definitely, we can also replace the arbitrary mesh motion with the real motion of the body at an infinitesimally preceding state. By doing so, the advantage is that it is then possible to linearize the constitutive equation relative to the preceding reference state so that the governing equation of the problem becomes linear partial differential equation for small deformation. This idea is similar to the well-known problem of small deformation superposed on finite deformation in the literature [5].

This remind us of the Lagrangian and the Eulerian descriptions in continuum mechanics and the one relative to the present configuration of the body in motion as the reference configuration, known as the *relative motion* description (see for example, [20, 9]). It is interesting to note that the above-mentioned idea is nothing but a Lagrangian formulation of thermomechanical problems in relative motion description. We shall call it the *relative Lagrangian* formulation, in contrast to the widely used (total or updated) Lagrangian and Eulerian formulations.

We can then propose a linear algorithm for large deformation based on relative Lagrangian formulation, by building up successive small incremental deformation problem at every time step in the deformation process. Roughly speaking, at each time step, the constitutive function is calculated at the present state of deformation which will be regarded as the reference configuration for the next state, and assuming the deformation to the next state is small, the constitutive function can be linearized. In this manner, it becomes a linear problem at each time step from one state to the next state successively with small deformations.

Numerical simulations for elastic bodies with this algorithm have been successfully implemented and compared with exact solutions for large deformations in pure shear [12] and bending of a rectangular block into a circular section [10]. In this paper, we extend the proposed method to viscoelastic solids and as an application, we consider the instability of a two-layered solid body of a denser elastic material on top of a lighter viscoelastic one. This problem is widely known to geophysicists in sediment-salt migration as salt diapirism. For some practical reasons in dealing with large deformations in solid bodies, oftentimes the problem has been treated as Rayleigh–Taylor instability in viscous fluids (see for example, [7, 8, 13]) instead of solid bodies. Obviously, although the instability phenomena may be quite similar for fluids and solids (as it says in rheology: in geological time, everything flows!), the distribution of the stress fields may be quite different in different classes of materials.

We will show in our numerical simulation with finite element method the formation of diapirs with viscoelastic solid models. The mesh of the calculation domain is updated as the body deforms at every step, however, up to very large deformation we have found that re-meshing is almost unnecessary.

After a brief introduction to kinematics in relative motion description in Sect. 2, linearization of constitutive equation and nearly incompressible bodies are considered in Sect. 3. A Mooney–Rivlin type viscoelastic solid material model is introduced as an example. In Sect. 4, an equilibrium boundary value problem in relative Lagrangian formulation is considered and its linearization and variational formulation are discussed. The new algorithm for large deformation with incremental loadings is proposed in Sect. 5. Since implementation of the algorithm for finite elements is not of our major concern in this paper, the numerical details are not included. Finally, two numerical simulations of salt migration are given as examples. The results are only qualitatively compared with the formation of salt domes in geophysics literature. No physical data are readily available for us to validate our simulations.

2 The relative motion description

Let κ_0 be a reference configuration of the body $\mathcal{B}$, and κ_t be its deformed configuration at the *present* time t, Let

$$\boldsymbol{x} = \chi(X, t), \qquad X \in \kappa_0(\mathcal{B}),$$

and

$$F(X, t) = \nabla_X(\chi(X, t)),$$

be the deformation and the deformation gradient from κ_0 to κ_t.

Now, at some time τ, consider the deformed configuration κ_τ, and

$$\boldsymbol{\xi} = \chi(X, \tau) := \boldsymbol{\xi}_t(\boldsymbol{x}, \tau) \in \kappa_\tau(\mathcal{B}), \qquad \boldsymbol{x} = \chi(X, t) \in \kappa_t(\mathcal{B}). \tag{1}$$

$\boldsymbol{\xi}_t(\boldsymbol{x}, \tau)$ is called the *relative motion* with respect to the present configuration at time t, and

$$F_t(\boldsymbol{x}, \tau) = \nabla_x \boldsymbol{\xi}_t(\boldsymbol{x}, \tau),$$

is called the relative deformation gradient (after common usage in continuum mechanics, see for example, [20, 9]). We also define the relative displacement vector as

$$\boldsymbol{u}(\boldsymbol{x}, \tau) = \boldsymbol{\xi}_t(\boldsymbol{x}, \tau) - \boldsymbol{x}, \tag{2}$$

and

$$H(\boldsymbol{x}, \tau) = \nabla_x \boldsymbol{u}(\boldsymbol{x}, \tau) = F_t(\boldsymbol{x}, \tau) - I, \tag{3}$$

is the relative displacement gradient at time τ with respect to the *present* configuration κ_t (emphasize, not κ_0), and I stands for the identity tensor.

Note that from (1),

$$\nabla_x \boldsymbol{\xi}_t(\boldsymbol{x}, \tau) = \nabla_X(\chi(X, \tau))\, \nabla_X(\chi(X, t))^{-1} = F(X, \tau) F(X, t)^{-1},$$

hence, by the use of (3) we have

$$H(\boldsymbol{x}, \tau) = F(X, \tau) F(X, t)^{-1} - I,$$

or simply as

$$F_t(\tau) = I + H(\tau) \quad \text{and} \quad F(\tau) = (I + H(\tau)) F(t). \tag{4}$$

Moreover, by taking the time derivative with respect to τ, it gives

$$\dot{F}(\tau) = \dot{H}(\tau) F(t). \tag{5}$$

In these expressions and hereafter, we shall often denote a function F as $F(t)$ to emphasize its value at time t when its spatial variable is self-evident.

We can represent the deformation and deformation gradient schematically in the following diagram:

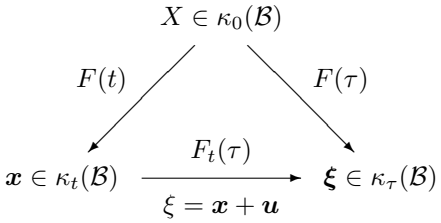

Furthermore, from (1) and (2) (or from the above diagram), we have

$$\boldsymbol{\chi}(X, \tau) = \boldsymbol{\chi}(X, t) + \boldsymbol{u}(\boldsymbol{\chi}(X, t), \tau). \tag{6}$$

By taking the derivatives with respect to τ, we obtain the velocity and the acceleration of the motion at time τ,

$$\dot{\boldsymbol{x}}(X, \tau) = \frac{\partial \boldsymbol{u}(\boldsymbol{x}, \tau)}{\partial \tau} = \dot{\boldsymbol{u}}(\boldsymbol{x}, \tau), \quad \ddot{\boldsymbol{x}}(X, \tau) = \ddot{\boldsymbol{u}}(\boldsymbol{x}, \tau). \tag{7}$$

Note that since $\boldsymbol{x} = \chi(X, t)$ is independent of τ, in relative motion description, the partial derivative with respect to τ keeping $\boldsymbol{x}$ fixed is nothing but the material time derivative.

Remark 3: On descriptions of motion

Recall that in *Lagrangian description*, a function $f(X,t)$ defined on the motion of a body is defined on the domain $\mathcal{B}_0 \times I\!R$, in the fixed reference configuration; while in *Eulerian description*, it is defined on the position x occupied by the body, $\widehat{f}(\boldsymbol{x},t)$. Note that the domain of the Eulerian description is not $\mathcal{B}_t \times I\!R$, but rather $\mathcal{B}_t \times \{t\}$.

On the other hand, one can also define the function on $\mathcal{B}_t \times I\!R$, at time τ relative to the present configuration, as if the function $f_t(\boldsymbol{x},\tau)$ is viewed at the instant τ from an observer attached to the body in its motion at the present time t. This is called the *relative motion description*.

The functions in Lagrangian, Eulerian and relative motion descriptions are related by

$$f(X,t) = \widehat{f}(\boldsymbol{x}(X,t),t), \qquad f(X,\tau) = f_t(\boldsymbol{x}(X,t),\tau).$$

Note that if $\tau = t$, the relative description reduces to the Eulerian description.

The advantage of using relative Lagrangian formulation is that it enable us to linearize constitutive equation relative to the present state and hence with a successive method of Euler's type, we can approximate the nonlinear constitutive functions for large deformations. □

3 Linearized constitutive equations

Let κ_0 be the preferred reference configuration of a viscoelastic body $\mathcal{B}$, and let the Cauchy stress $T(X,t)$ be given by the constitutive equation in the configuration κ_0,

$$T(X,t) = \mathcal{T}(F(X,t), \dot{F}(X,t)). \tag{8}$$

For large deformations, the constitutive function $\mathcal{T}$ is generally a nonlinear function of the deformation gradient F.

We shall regard the present configuration κ_t as an *updated* reference configuration, and consider a small deformation relative to the present state $\kappa_t(\mathcal{B})$ at time $\tau = t + \Delta t$, for small enough time interval Δt. In other words, we shall assume that the relative displacement gradient H is small, $|H| \ll 1$, so that we can linearize the constitutive equation (8) at time τ relative to the updated reference configuration at time t, namely,

$$\begin{aligned} T(\tau) &= \mathcal{T}(F(\tau), \dot{F}(\tau)) = \mathcal{T}(F(t),0) \\ &\quad + \partial_F \mathcal{T}(F(t),0)[F(\tau) - F(t)] + \partial_{\dot{F}} \mathcal{T}(F(t),0)[\dot{F}(\tau)] + o(2), \end{aligned}$$

or by the use of (5),

$$T(\tau) = T_e(t) + \partial_F \mathcal{T}(F(t),0)[H(\tau)F(t)] + \partial_{\dot{F}} \mathcal{T}(F(t),0)[\dot{H}(\tau)F(t)] + o(2).$$

where

$$T_e(t) = \mathcal{T}(F(t),0)$$

is the elastic Cauchy stress at the present time t and $o(2)$ represents higher order terms in the small displacement gradient $|H|$.

The linearized constitutive equation can now be written as

$$T(\tau) = T_e(t) + L(F(t))[H(\tau)] + M(F(t))[\dot{H}(\tau)], \tag{9}$$

where

$$L(F)[H] := \partial_F \mathcal{T}(F,0)[HF], \qquad M(F)[\dot{H}] := \partial_{\dot{F}} \mathcal{T}(F,0)[\dot{H}F], \tag{10}$$

define the fourth order elasticity tensor $L(F)$ and viscosity tensor $M(F)$ relative to the present configuration κ_t.

The above general definition of the elasticity and the viscosity tensors for any constitutive class of viscoelastic materials $T = \mathcal{T}(F,\dot{F})$, relative to the updated present configuration, will be explicitly determined in the following sections for a particular class, namely a Mooney–Rivlin type materials.

3.1 Compressible and nearly incompressible bodies

For a viscoelastic body, the constitutive equation (8) relative to the preferred reference configuration κ_0 can be written as

$$T = \mathcal{T}(F, \dot{F}) = -p(F)I + \widetilde{\mathcal{T}}(F, \dot{F}). \tag{11}$$

However, for an incompressible body, the pressure p depends also on the boundary conditions, and because it cannot be determined from the deformation of the body alone, it is called an *indeterminate pressure*, which is an independent variable in addition to the displacement vector variable for boundary value problems.

For compressible bodies, we shall assume that the pressure depend on the deformation gradient only through the determinant, or by the use of the mass balance, depend only on the mass density,

$$p = \hat{p}(\det F) = p(\rho), \qquad \rho = \frac{\rho_0}{\det F},$$

where ρ_0 is the mass density in the reference configuration κ_0. We have

$$\begin{aligned}\rho(\tau) - \rho(t) &= \rho_0(\det F(\tau)^{-1} - \det F(t)^{-1}) = \rho(t)(\det(F(\tau)^{-1}F(t)) - 1)\\ &= \rho(t)(\det(I + H(\tau))^{-1} - 1) = -\rho(t)\,\mathrm{tr}\,H(\tau) + o(2),\end{aligned}$$

in which the relation (4) has been used.

Therefore, it follows that

$$p(\tau) - p(t) = \Big(\frac{dp}{d\rho}\Big)_t(\rho(\tau) - \rho(t)) + o(2) = -\Big(\rho\,\frac{dp}{d\rho}\Big)_t\,\mathrm{tr}\,H(\tau) + o(2),$$

or

$$p(\tau) = p(t) - \beta\,\mathrm{tr}\,H(\tau) + o(2), \tag{12}$$

where $\beta := \big(\rho\,\frac{dp}{d\rho}\big)_t$ is a material parameter evaluated at the present time t.

From (11) and (4), let

$$C(F(t))[H(\tau)] := \partial_F\widetilde{\mathcal{T}}(F(t), 0)[F(\tau) - F(t)] = \partial_F\widetilde{\mathcal{T}}(F(t), 0)[H(\tau)F(t)],$$

then from $(10)_1$, the elasticity tensor becomes

$$L(F)[H] = \beta(\mathrm{tr}\,H)I + C(F)[H]. \tag{13}$$

We call a body nearly incompressible if its density is nearly insensitive to the change of pressure. Therefore, if we regard the density as a function of pressure, $\rho = \rho(p)$, then its derivative with respect to the pressure is nearly zero. In other words, for nearly incompressible bodies, we shall assume that β is a material parameter much greater than 1,

$$\beta \gg 1. \tag{14}$$

Note that for compressible or nearly incompressible body, the elasticity tensor does not contain the pressure explicitly. It is only a function of the deformation gradient and the material parameter β at the present time t.

3.2 A viscoelastic material model

The constitutive equation $T = \mathcal{T}(F, \dot{F})$ of an viscoelastic material should satisfy the conditions of material symmetry and material objectivity, respectively,

$$\begin{aligned}&\mathcal{T}(FG, \dot{F}G) = \mathcal{T}(F, \dot{F}),\\ &\mathcal{T}(QF, (QF)^{\cdot}) = Q\,\mathcal{T}(F, \dot{F})Q^T,\end{aligned}$$

for any orthogonal transformation Q and any G belonging to the symmetry group of the material. For isotropic materials, the symmetry group is the orthogonal group. Therefore, for any deformation gradient with its polar decomposition $F = VR$, where R is orthogonal and V is positive definite, by taking $G = R^T$, we obtain from the symmetry condition that

$$\mathcal{T}(F, \dot{F}) = \mathcal{T}((VR)R^T, \dot{F}F^{-1}(VR)R^T) = \mathcal{T}(V, LV) := \widehat{\mathcal{T}}(B, L),$$

where $L = \dot{F}F^{-1}$ is the spatial velocity gradient and $B = V^2 = FF^T$ is the left Cauchy–Green strain tensor. The objectivity condition can then be written as

$$\widehat{\mathcal{T}}(QBQ^T, QLQ^T + \dot{Q}Q^T) = Q\,\widehat{\mathcal{T}}(B, L)Q^T.$$

Let $L = D + W$ where D is the symmetric part and W the skew-symmetric part of the velocity gradient. By taking the orthogonal transformation $Q(s) = \exp((t-s)W)$, we have $Q(t) = I$ and $\dot{Q}(t) = -W$, the above equation reduces to $\widehat{\mathcal{T}}(B, L-W) = \widehat{\mathcal{T}}(B, L)$. Therefore the constitutive function $\widehat{\mathcal{T}}$ reduces to

$$\mathcal{T}(F, \dot{F}) = \widehat{\mathcal{T}}(B, D),$$

and moreover, the above objectivity condition requires that $\widehat{\mathcal{T}}(B, D)$ be an isotropic function of two symmetric tensor variables, i.e.,

$$\widehat{\mathcal{T}}(QBQ^T, QDQ^T) = Q\,\widehat{\mathcal{T}}(B, D)Q^T,$$

for any orthogonal transformation Q. General representation of such isotropic functions are well-known (see for example, [9]). In particular, we shall lay down the following constitutive equation for an isotropic viscoelastic material,

$$\begin{aligned} &T = \mathcal{T}(F, \dot{F}) = -p(F)I + \widetilde{\mathcal{T}}(F, \dot{F}), \qquad \text{where} \\ &\widetilde{\mathcal{T}}(F, \dot{F}) = s_1 B + s_2 B^{-1} + \lambda(\operatorname{tr} D)I + 2\mu_1 D + \mu_2(DB + BD) + \mu_3(DB^{-1} + B^{-1}D). \end{aligned} \tag{15}$$

The material parameters s_1 through μ_3 are assumed to be constants. This material model will be referred to as a *Mooney–Rivlin type isotropic viscoelastic solid*, since the elastic part of the constitutive equation represents the well-known Mooney–Rivlin isotropic elastic solid in nonlinear elasticity (see [20, 9, 11]). Note that this constitutive equation contains only linear terms in D (see also [6]). Therefore, it would be appropriate for large deformations with small strain rate.

After taking the gradients of $\widetilde{\mathcal{T}}(F, \dot{F})$ with respect to F at $(F, 0)$, we have

$$C(F)[H] = s_1(HB + BH^T) - s_2(B^{-1}H + H^T B^{-1}),$$

which by (13), gives the elasticity tensor

$$L(F)[H] = \beta(\operatorname{tr} H)I + s_1(HB + BH^T) - s_2(B^{-1}H + H^T B^{-1}), \tag{16}$$

and with respect to $\dot{F}$, we obtain

$$M(F)[\dot{H}] = \lambda(\operatorname{tr} \dot{H})I + M_0(\dot{H} + \dot{H}^T) + (\dot{H} + \dot{H}^T)M_0, \tag{17}$$

where

$$M_0 := \frac{1}{2}(\mu_1 I + \mu_2 B + \mu_3 B^{-1}).$$

From (9), we have

$$T(\tau) = T_e(t) + L(F(t))[H(\tau)] + M(F(t))[\dot{H}(\tau)]. \tag{18}$$

For relative Lagrangian formulation, we shall need the (first) Piola-Kirchhoff stress tensor at time τ relative to the present configuration at time t, denoted by $T_t(\tau)$, and given by

$$\begin{aligned} T_t(\tau) &:= \det F_t(\tau)\, T(\tau) F_t(\tau)^{-T} = \det(I+H)\, T(\tau)(I+H)^{-T} \\ &= \det(I+H)\big(T_e(t) + L(F)[H] + M(F)[\dot{H}]\big)(I+H)^{-T} \\ &= (I + \operatorname{tr} H)\big(T_e(t) + L(F)[H] + M(F)[\dot{H}]\big)(I - H^T) + o(2) \\ &= T_e(t) + (\operatorname{tr} H) T_e(t) - T_e(t) H^T + L(F)[H] + M(F)[\dot{H}] + o(2). \end{aligned}$$

We can write the linearized Piola-Kirchhoff stress as

$$\begin{aligned} T_t(\tau) = T_e(t) &+ (\operatorname{tr} H(\tau)) T_e(t) - T_e(t) H(\tau)^T \\ &+ L(F(t))[H(\tau)] + M(F(t))[\dot{H}(\tau)]. \end{aligned}$$

Note that when $\tau \to t$, $H \to 0$, and hence $T_t(\tau) \to T(t)$, therefore, the Piola-Kirchhoff stress, becomes the Cauchy stress at the present time t.

We can also write

$$T_t(\tau) = T_e(t) + K(F(t), T_e(t))[H(\tau)] + M(F(t))[\dot{H}(\tau)], \tag{19}$$

where the Piola-Kirchhoff elasticity tensor is defined as

$$K(F, T_e)[H] := (\operatorname{tr} H) T_e - T_e H^T + L(F)[H]. \tag{20}$$

In numerical examples presented later, the material is assumed to be of Mooney–Rivlin type and these relations will be used.

4 Boundary value problem

Let κ be a reference configuration of the body $\mathcal{B}$, then in the Lagrangian formulation, we can write the equation of motion at time τ as

$$\rho_\kappa(\boldsymbol{X})\ddot{\boldsymbol{x}}(\boldsymbol{X}, \tau) - \operatorname{Div} T_\kappa(\boldsymbol{X}, \tau) = \rho_\kappa(\boldsymbol{X})\boldsymbol{g}(\boldsymbol{X}, \tau), \qquad \boldsymbol{X} \in \kappa(\mathcal{B}),$$

where $T_\kappa(\tau)$ is the Piola–Kirchhoff stress tensor at time τ relative to the reference configuration κ, and $\boldsymbol{g}(\tau)$ is the body force. The operator (Div) stands for the divergence with respect to the coordinate system $(\boldsymbol{X})$ in $\kappa(\mathcal{B})$, and the overhead dot $(\dot{\cdot})$ is the material time derivative with respect to time variable τ.

Instead of the fixed reference configuration κ, we can rewrite the equation relative to the configuration κ_t at the present time t as the reference configuration. By a simple substitution, it becomes

$$\rho(\boldsymbol{x}, t)\ddot{\boldsymbol{x}}(\boldsymbol{x}, \tau) - \operatorname{div} T_t(\boldsymbol{x}, \tau) = \rho(\boldsymbol{x}, t)\boldsymbol{g}(\boldsymbol{x}, \tau), \qquad \boldsymbol{x} \in \kappa_t(\mathcal{B}),$$

where $T_t(\tau) = T_{\kappa_t}(\tau)$ is the Piola–Kirchhoff stress tensor at time τ relative to the present configuration κ_t. The operator (div) stands for the divergence with respect to the coordinate system $(\boldsymbol{x})$ in the present configuration.

As we have stated in Remark 3 previously, this is a formulation of the equation of motion in the relative motion description. We call this a *relative Lagrangian* formulation. In this formulation, the time variable of the problem is the instant τ, which may be regarded as the *next instant* from the present time. Now we can consider the following boundary value problem in the relative Lagrangian formulation:

Let $\Omega = \kappa_t(\mathcal{B}) \subset I\!R^3$ be the region occupied by the body at the present time t, and $\partial\Omega = \Gamma_1 \cup \Gamma_2$, and $\boldsymbol{n}_\kappa$ be the exterior unit normal to $\partial\Omega$. At the next instant $\tau > t$,

we consider the boundary value problem with the present state at time t as the reference configuration, given by

$$\begin{cases} \rho(t)\ddot{\boldsymbol{u}}(\tau) - \operatorname{div} T_t(\tau) = \rho(t)\boldsymbol{g}(\tau), & \text{in } \Omega, \\ T_t(\tau)\,\boldsymbol{n}_\kappa = \boldsymbol{f}(\tau), & \text{on } \Gamma_1, \\ \boldsymbol{u}(\tau)\cdot\boldsymbol{n}_\kappa = 0, & \text{on } \Gamma_2, \\ T_t(\tau)\,\boldsymbol{n}_\kappa \times \boldsymbol{n}_\kappa = 0, & \text{on } \Gamma_2, \\ \boldsymbol{u}(t) = 0, \quad \dot{\boldsymbol{u}}(t) = \boldsymbol{v}_0, & \text{in } \Omega, \end{cases} \tag{21}$$

where $\boldsymbol{u}(\boldsymbol{x},\tau)$ is the relative displacement vector and from (7), $\ddot{\boldsymbol{x}}(\tau) = \ddot{u}(\tau)$. The body is subjected to the body force $\boldsymbol{g}(\boldsymbol{x},\tau)$ and the surface traction $\boldsymbol{f}(\boldsymbol{x},\tau)$. Note that the initial condition $\boldsymbol{u}(\boldsymbol{x},t) = 0$ is the consequence of the relation (6).

Since $T_t(\tau)\boldsymbol{n}_\kappa \times \boldsymbol{n}_\kappa = 0$ implies that the surface traction $T_t(\tau)\boldsymbol{n}_\kappa$ is in the direction of the normal, the last boundary condition in (21) states that the tangential component of the surface traction $T_t(\tau)\boldsymbol{n}_\kappa$ vanishes on Γ_2. In other words, the boundary Γ_2 is a roller-supported boundary.

4.1 Linearized boundary value problem

We shall assume that at the present time t, the deformation gradient F with respect to the preferred reference configuration κ_0 and the Cauchy stress T are known, and that $\tau = t + \Delta t$ with small enough Δt. If we denote the linear operator $\mathcal{P}(\mathcal{F})$ by

$$\mathcal{P}(F(t))[\boldsymbol{u}(\tau)] := K(F(t), T_e(t))[\nabla \boldsymbol{u}(\tau)] + M(F(t))[\nabla \dot{\boldsymbol{u}}(\tau)],$$

then from (19), the equation of motion and the traction boundary condition in (21) can be written as

$$\begin{aligned} \rho(t)\ddot{\boldsymbol{u}}(\tau) - \operatorname{div}(\mathcal{P}(F(t))[\boldsymbol{u}(\tau)]) = \rho(t)\boldsymbol{g}(\tau) + \operatorname{div} T_e(t) = \rho(t)(\boldsymbol{g}(\tau) - \boldsymbol{g}(t)) \quad \text{in } \Omega, \\ \mathcal{P}(F(t))[\boldsymbol{u}(\tau)]\boldsymbol{n}_\kappa = \boldsymbol{f}(\tau) - T_e(t)\boldsymbol{n}_\kappa = \boldsymbol{f}(\tau) - \boldsymbol{f}(t) \quad \text{on } \Gamma_1, \end{aligned} \tag{22}$$

which is a linear system for the relative displacement vector $\boldsymbol{u}(\boldsymbol{x},\tau)$. The right hand sides represent the incremental forces for the time interval Δt, which are known functions. Incremental features of the present formulation will be discussed again in Sect. 5.1.

The idea of formulating the boundary value problem in the form (21) for small time increment is similar to the theory of small deformations superposed on finite deformations (see [5, 20]), and the problem can be treated as one in linear elasticity, with the value of the elasticity tensor updated at the present state instead of a constant.

4.2 Variational formulation

We shall restrict our attention to equilibrium problems or quasi-static problems, for which the acceleration can be neglected, in the following discussions and numerical examples.

The boundary value problem (21) can be formulated as a variational problem. Let us consider the Sobolev space of vector valued functions on Ω,

$$H^1(\Omega) = \{\boldsymbol{v} : \Omega \to I\!R^3 \mid \boldsymbol{v},\, \nabla \boldsymbol{v} \in L^2(\Omega)\}$$

and the subspace

$$V = \{\boldsymbol{v} \in H^1(\Omega) \mid \boldsymbol{v}\cdot\boldsymbol{n}_\kappa = 0 \text{ on } \Gamma_2\}.$$

Taking the inner product of the equation (22) with a vector $\boldsymbol{w} \in V$ and integrating over the domain Ω, we obtain, after integration by parts,

$$\begin{aligned} &\int_\Omega \Big(K[\nabla \boldsymbol{u}(\tau)] + M[\nabla \dot{\boldsymbol{u}}(\tau)]\Big) \cdot \nabla \boldsymbol{w}\, dv \\ &\qquad = \int_\Omega \rho(t)\boldsymbol{g}(\tau)\cdot\boldsymbol{w}\, dv - \int_\Omega T_e(t)\cdot\nabla\boldsymbol{w}\, dv + \int_{\partial\Omega} T_t(\tau)\boldsymbol{n}_\kappa\cdot\boldsymbol{w}\, da, \end{aligned}$$

where the relation (19) is used and dot $(\cdot)$ represents the inner product between two vectors as well as the inner product between two second order tensors, i.e., $A \cdot B = \mathrm{tr}(AB^T)$.

Since $\boldsymbol{w} \in V$, $\boldsymbol{w} \cdot \boldsymbol{n}_\kappa = 0$, by the boundary conditions the surface integral on the right hand side becomes

$$\int_{\partial\Omega} T_t(\tau)\boldsymbol{n}_\kappa \cdot \boldsymbol{w}\, da = \int_{\Gamma_1} \boldsymbol{f}(\tau) \cdot \boldsymbol{w}\, da.$$

Therefore, if we define the following bilinear forms

$$\begin{aligned} \mathcal{L}(\boldsymbol{w}, \boldsymbol{u}(\tau)) &:= \int_\Omega K[\nabla \boldsymbol{u}(\tau)] \cdot \nabla \boldsymbol{w}\, dv, \\ \mathcal{M}(\boldsymbol{w}, \dot{\boldsymbol{u}}(\tau)) &:= \int_\Omega M[\nabla \dot{\boldsymbol{u}}(\tau)] \cdot \nabla \boldsymbol{w}\, dv, \end{aligned} \tag{23}$$

and the linear form,

$$\mathcal{N}(\boldsymbol{w}) := \int_\Omega \rho(t)\boldsymbol{g}(\tau) \cdot \boldsymbol{w}\, dv + \int_{\Gamma_1} \boldsymbol{f}(\tau) \cdot \boldsymbol{w}\, da - \int_\Omega T_e(t) \cdot \nabla \boldsymbol{w}\, dv, \tag{24}$$

then the variational problem is to find the solution vector $\boldsymbol{u}(\tau) \in V$ such that

$$\mathcal{L}(\boldsymbol{w}, \boldsymbol{u}(\tau)) + \mathcal{M}(\boldsymbol{w}, \dot{\boldsymbol{u}}(\tau)) = \mathcal{N}(\boldsymbol{w}) \quad \forall\, \boldsymbol{w} \in V. \tag{25}$$

Note that from the initial condition in (21), $\boldsymbol{u}(\boldsymbol{x}, t) = 0$, we can approximate

$$\dot{\boldsymbol{u}}(\tau) \approx \frac{1}{\Delta t}\, \boldsymbol{u}(\tau),$$

and hence restate the variational problem as: Find the solution vector $\boldsymbol{u}(\tau) \in V$ such that

$$\mathcal{K}(\boldsymbol{w}, \boldsymbol{u}(\tau)) = \mathcal{N}(\boldsymbol{w}) \quad \forall\, \boldsymbol{w} \in V, \tag{26}$$

where

$$\mathcal{K}(\boldsymbol{w}, \boldsymbol{u}) := \mathcal{L}(\boldsymbol{w}, \boldsymbol{u}) + \frac{1}{\Delta t}\mathcal{M}(\boldsymbol{w}, \boldsymbol{u}).$$

The variational problem depends on the elasticity and viscosity tensor at the updated present state. Mathematical analysis of requirements at the present state for existence and uniqueness of solution will be presented in a forthcoming paper [3]. In general, non-existence or non-uniqueness may occurred if such requirements are not fulfilled.

For numerical solutions of the variational equation, finite element method will be used.

5 Algorithm of successive linear approximation

Recall the Euler method of solving differential equation, say $\dot{y} = f(t)$, that for a discrete time axis, $\cdots < t_{n-1} < t_n < t_{n+1} < \cdots$, and $y(t_n) = y_n$, the solution curve can be constructed by $y_{n+1} = y_n + f(t_n)\Delta t$, where $f(t_n)$ is the tangent of the solution curve at t_n. We can use a similar strategy for solving problems of large deformation, by solving linear variational problem stated in (26).

We consider a discrete time axis, $t_0 < \cdots < t_n < t_{n+1} < \cdots$ with small enough time increment Δt. Let κ_{t_n} be the configuration of the body at the instant t_n and

$$\boldsymbol{x}_n = \chi(X, t_n) \in \kappa_{t_n}(\mathcal{B}) \quad \text{for} \quad X \in \kappa_0(\mathcal{B}), \quad \kappa_0 = \kappa_{t_0}.$$

Let the elastic Cauchy stress $T_e(\boldsymbol{x}_n, t_n)$ and the deformation gradient $F(\boldsymbol{x}_n, t_n)$ relative to the preferred configuration κ_0 at the present time $t = t_n$ be known. The boundary value problem (21) at the instant $\tau = t_{n+1}$ with the body force $\boldsymbol{b}(\boldsymbol{x}_n, t_{n+1})$ and the surface traction $\boldsymbol{f}(\boldsymbol{x}_n, t_{n+1})$ in relative Lagrangian formulation with respect to the present configuration κ_{t_n},

can now be solved numerically as a problem in linear elasticity for the relative displacement field $\boldsymbol{u}(\boldsymbol{x}_n, t_{n+1})$ from the present state at t_n.

After solving the problem (21) at t_n, the configuration $\kappa_{t_{n+1}}$ can be regarded as the reference configuration at the updated present time t_{n+1} from the displacement field, i.e.,

$$\boldsymbol{x}_{n+1} = \chi(X, t_{n+1}) = \boldsymbol{x}_n + \boldsymbol{u}(\boldsymbol{x}_n, t_{n+1}),$$

while the deformation gradient

$$F(\boldsymbol{x}_{n+1}, t_{n+1}) = \big(I + \nabla \boldsymbol{u}(\boldsymbol{x}_n, t_{n+1})\big) F(\boldsymbol{x}_n, t_n)$$

and the elastic Cauchy stress $T_e(\boldsymbol{x}_{n+1}, t_{n+1})$ can be calculated from (18) at t_{n+1} so that the relative Lagrangian formulation of the problem in the form (21), with the body force $\boldsymbol{b}(\boldsymbol{x}_{n+1}, t_{n+2})$ and the surface traction $\boldsymbol{f}(\boldsymbol{x}_{n+1}, t_{n+2})$, can proceed again from the updated referential configuration $\kappa_{t_{n+1}}$. This numerical algorithm will be referred to as the *successive relative lagrangian formulation of linear approximation*, or simply as the algorithm of *Successive Linear Approximation* (SLA). The updating algorithm can be represented in the following schematic diagram:

$$\begin{array}{ccccc}
\kappa_{t_0}(\mathcal{B}) & \xrightarrow[\text{deforms}]{\text{fintely}} & \begin{array}{c}\kappa_t = \kappa_{t_n} \\ \kappa_{t_n}(\mathcal{B})\end{array} & \xrightarrow{\text{BVP}} & \begin{array}{c}\kappa_\tau = \kappa_{t_{n+1}} \\ \kappa_{t_{n+1}}(\mathcal{B})\end{array} \\
 & & & & \\
 & & \text{update} & & \Downarrow \\
 & & & & \\
 & & \begin{array}{c}\kappa_t = \kappa_{t_{n+1}} \\ \kappa_{t_{n+1}}(\mathcal{B})\end{array} & \xrightarrow{\text{BVP}} & \begin{array}{c}\kappa_\tau = \kappa_{t_{n+2}} \\ \kappa_{t_{n+2}}(\mathcal{B})\end{array} \\
 & & & & \\
 & & & \text{update} & \Downarrow \\
 & & & & \\
 & & & & \begin{array}{c}\kappa_t = \kappa_{t_{n+2}} \\ \cdots\cdots\end{array}
\end{array}$$

where BVP stands for the linear boundary value problem formulated in (21) to be solved successively after each update as shown in the above scheme, and the process starts with $\kappa_t = \kappa_{t_0}$ which is the initial reference configuration at $n = 0$.

5.1 Incremental loadings

Note that the force term $\mathcal{N}(\boldsymbol{w})$ in the variational equation (26) defined in (24) is, in fact, a small quantity of the order of the time increment Δt. Therefore, the method of SLA can be regarded as an incremental method. Here we shall emphasize the incremental features of the boundary value problem (21).

For convenience, we shall denote the time dependence on t_n as subindex n or simply as n. For example, we write the Cauchy stress $T(t_n) = T_n$ and the elastic Cauchy stress $T_e(t_n) = T_e(n)$, and we have

$$T_n = \mathcal{T}(F_n, \dot{F}_n) = \mathcal{T}(F_n, 0) + \partial_{\dot{F}} \mathcal{T}(F_n, 0)[\dot{F}_n] = T_e(n) + \partial_{\dot{F}} \mathcal{T}(F_n, 0)[\dot{F}_n]\,. \tag{27}$$

Now, we can rewrite the variational equation (26) as,

$$\mathcal{K}(\boldsymbol{w}, \boldsymbol{u}_{n+1}) = \mathcal{N}(\boldsymbol{w}, n) \quad \forall\, \boldsymbol{w} \in V, \tag{28}$$

where, from (24), the force term is given by

$$\mathcal{N}(\boldsymbol{w}, n) = \int_\Omega \rho_n \boldsymbol{g}_{n+1} \cdot \boldsymbol{w}\, dv + \int_{\Gamma_1} \boldsymbol{f}_{n+1} \cdot \boldsymbol{w}\, da - \int_\Omega T_e(n) \cdot \nabla \boldsymbol{w}\, dv. \tag{29}$$

Note that by (27), it follows that

$$\int_\Omega T_e(n)\cdot\nabla\boldsymbol{w}\,dv=\int_\Omega T_n\cdot\nabla\boldsymbol{w}\,dv-\int_\Omega\partial_{\dot F}\mathcal{T}(F_n,0)[\dot F_n]\cdot\nabla\boldsymbol{w}\,dv, \tag{30}$$

and

$$\int_\Omega T_n\cdot\nabla\boldsymbol{w}\,dv=\int_{\partial\Omega}T_n\boldsymbol{n}_\kappa\cdot\boldsymbol{w}\,dv-\int_\Omega\operatorname{div}T_n\cdot\boldsymbol{w}\,dv.$$

On the other hand, knowing that $T_{t_n}(t_n)=T_n$ is the Cauchy stress at t_n, from (21) we have the following boundary value problem at the present time t_n,

$$\begin{cases}-\operatorname{div}T_n=\rho_n\boldsymbol{g}_n, & \text{in }\Omega,\\ T_n\boldsymbol{n}_\kappa=\boldsymbol{f}_n, & \text{on }\Gamma_1,\\ T_n\boldsymbol{n}_\kappa\times\boldsymbol{n}_\kappa=0, & \text{on }\Gamma_2,\end{cases}$$

which leads to

$$\int_\Omega T_n\cdot\nabla\boldsymbol{w}\,dv=\int_{\Gamma_1}\boldsymbol{f}_n\cdot\boldsymbol{w}\,dv+\int_\Omega\rho_n\boldsymbol{g}_n\cdot\boldsymbol{w}\,dv. \tag{31}$$

Combing (29), (30), and (31), we obtain

$$\mathcal{N}(\boldsymbol{w},n)=I_1(\boldsymbol{w},n)+I_2(\boldsymbol{w},n)+I_3(\boldsymbol{w},n), \tag{32}$$

which contains three types of loading for the variational equation (28), namely,

$$\begin{aligned}I_1(\boldsymbol{w},n)&=\int_\Omega\rho_n(\boldsymbol{g}_{n+1}-\boldsymbol{g}_n)\cdot\boldsymbol{w}\,dv,\\ I_2(\boldsymbol{w},n)&=\int_{\Gamma_1}(\boldsymbol{f}_{n+1}-\boldsymbol{f}_n)\cdot\boldsymbol{w}\,da,\\ I_3(\boldsymbol{w},n)&=\int_\Omega\partial_{\dot F}\mathcal{T}(F_n,0)[\dot F_n]\cdot\nabla\boldsymbol{w}\,dv.\end{aligned} \tag{33}$$

The integral I_1 represents the incremental body force and I_2 is the incremental surface traction between time steps t_n and t_{n+1}. The third one I_3 is due to the viscous effect of the material body.

5.2 Incremental approximation for large deformations

If we assume that the functions $\boldsymbol{g}(\boldsymbol{x},t)$ and $\boldsymbol{f}(\boldsymbol{x},t)$ are smooth in t, then their increments, $\boldsymbol{g}_{n+1}-\boldsymbol{g}_n$ and $\boldsymbol{f}_{n+1}-\boldsymbol{f}_n$, are of the order of $\Delta t=t_{n+1}-t_n$, and since the variational equation is linear, the solution vector $\boldsymbol{u}(\boldsymbol{x},t_{n+1})$ is also of the same order. For elastic material bodies, these are the two possible types of incremental loading.

Starting from an initial solution and applying the method of SLA with proper loading conditions at each time step, the problem of large deformation can be obtained. Numerical examples employing the SLA method for incremental surface traction of pure shear and of gradually bending a rectangular block into a circular section have been considered in [12, 10] for Mooney–Rivlin elastic materials.

For viscoelastic material bodies, there is a possible incremental loading due to the integral I_3. To see this, we shall consider the case without surface traction $\boldsymbol{f}=0$ and time-independent body force $\boldsymbol{g}$ so that $I_1=I_2=0$, hence the integral I_3 is the only possible incremental loading.

To begin with, for $n=0$, assume that at the initial time t_0, we have a static equilibrium solution so that we have the initial conditions: $F_0=I$ and $\dot F_0=0$. Therefore, from (28), (32) and $(33)_3$, we have

$$\mathcal{K}(\boldsymbol{w},\boldsymbol{u}_1)=I_3(\boldsymbol{w},0)=0,\qquad\forall\,\boldsymbol{w}\in V,$$

which implies that the solution vector $\boldsymbol{u}_1(\boldsymbol{x}) = 0$. Consequently, $\dot{\boldsymbol{u}}_1 = \frac{1}{\Delta t}\boldsymbol{u}_1 = 0$ and $\dot{H}_1 = \nabla\dot{\boldsymbol{u}}_1 = 0$. Then, from (5), $\dot{F}_1 = \dot{H}_1 F_0 = 0$, which, in turn, leads to

$$\mathcal{K}(\boldsymbol{w}, \boldsymbol{u}_2) = I_3(\boldsymbol{w}, 1) = 0, \qquad \forall\, \boldsymbol{w} \in V,$$

and implies that $\boldsymbol{u}_2$ must also vanish and so on. In other words, if the initial solution is an equilibrium solution, the solution remains valid for all time. However, this conclusion may not be true since the initial solution may not be a stable equilibrium solution in general.

Therefore, in order to study the stability, a small perturbation of the initial solution is needed so that $\boldsymbol{u}_1 \neq 0$, and hence $I_3(\boldsymbol{w}, 1) \neq 0$, to trigger the successive evolution of deformations. Two such examples are considered in the following sections.

6 Salt migration

As an example of large deformation, we shall consider a body consisting of two different layers initially, with the mass density of the upper layer, the overburden sediment, greater than that of the bottom layer, the rock salt.

In a similar situation for viscous fluids, the inversion of density leads to the so-called Rayleigh–Taylor instability due to buoyancy effect of gravity. In the numerical simulation by the use of SLA method, we shall present the results confirming the existence of similar instability for viscoelastic solid bodies.

Consider a body consisting of two layers of elastic and viscoelastic solids as shown in Fig. 1. The body is under the action of gravity $\boldsymbol{g}$, and $\rho_1 < \rho_2$. The upper boundary Γ_1 is

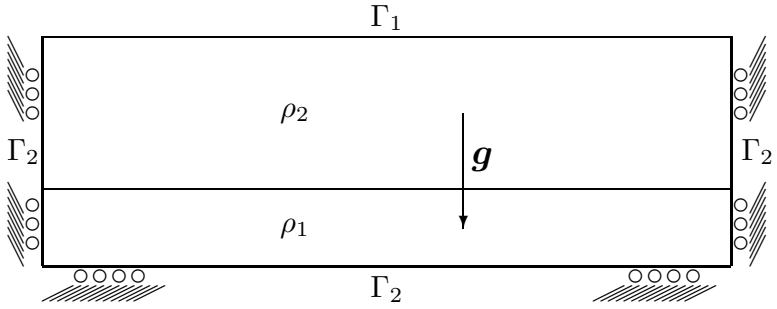

Figure 1: Boundary conditions and initial state.

traction-free, the others Γ_2 are roller-supported.

The initial state under the action of gravity is an equilibrium state. However, since the bottom layer is lighter than the upper one, in the case of viscous fluid, it leads to the well-known Rayleigh–Taylor instability. We shall show that similar instability exists for solid bodies in our numerical simulations of salt migration in sediment-salt tectonics, in the sense that the initial equilibrium state of sediment-salt system can not be maintained under any small perturbation.

For illustrative purpose, we shall present numerical simulations in a two-dimensional domain for a Mooney–Rivlin type material. The proposed method has been applied to three-dimensional domain and some different classes of viscoelastic solid bodies with similar results.

6.1 Formation of a salt diapir

In this example we consider formation of a salt diapir initiated by a small perturbation at a very small region centered at the salt-sediment interface.

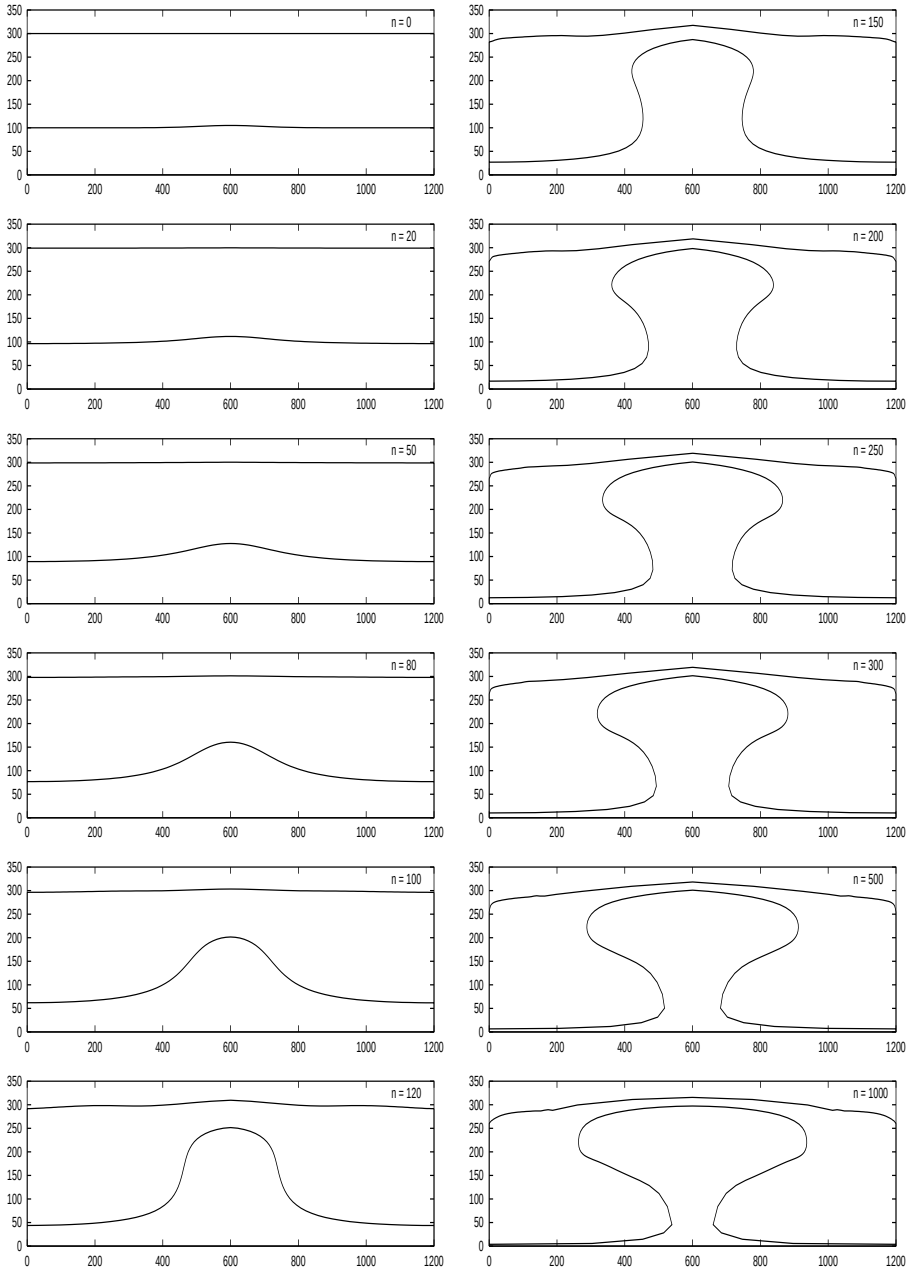

Figure 2: Migration of salt diapirism initiated by a small perturbation at the center of salt-sediment interface. The sequence represents the formation of a diapir during 100 million years ($t = n\,\Delta t$).

- The dimension of the initial state is: length = 1,200 m, height of salt layer = 100 m, height of sediment layer = 200 m. Initial rectangular mesh (80×30).
- The material parameters for rock salt are:
  $\rho_0 = 2.2\times10^3$ Kg/m^3, $s_1 = 0$, $s_2 = -0.2\times10^3$ Pa,
  $\lambda = -10.0\times10^3$ Pa Ma, $\mu_1 = 15.0\times10^3$ Pa Ma, $\mu_2 = \mu_3 = 0$, $\beta = 10^9$ Pa.
- The material parameters for overburden sediment are:
  $\rho_0 = 3.0\times10^3$ Kg/m^3, $s_1 = 2.5\times10^3$ Pa, $s_2 = -7.5\times10^3$ Pa,
  $\lambda = \mu_1 = \mu_2 = \mu_3 = 0$, $\beta = 10^9$ Pa.
- The incremental time: $\Delta t = 0.1$ Ma.

The material data are of convenient choice for demonstration only. No attempt has been made to match the data to real properties of relevant materials.

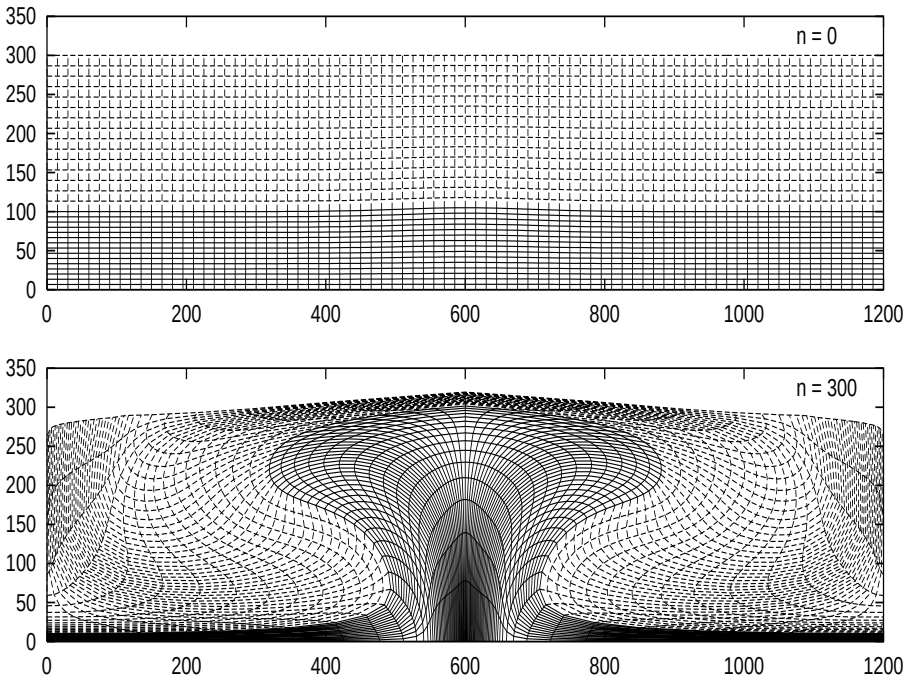

Figure 3: Original mesh and the deformed mesh at $n = 300$.

In Fig. 2, various stages of migration of the salt-sediment interface are shown, where n is the time step. One can easily see the formation of salt diapir as time step increases. The effect is primarily due to buoyancy force of density inversion. The diapir reaches its maximum height at about 20 Ma (million years) at $n = 200$ with almost no change afterward as the diapir becomes mature. The formation of diapir is a result of very large deformation of the initial mesh as can be seen from Fig. 3 at $n = 300$. The deformed mesh is quite similar to the experimental results of silicone putty model of a diapir formed by spinning the model in a centrifuge by Dixon [4]. Moreover, since the material data are conveniently chosen, and no experimental data of the stress fields are readily available for comparison, we do not show the stress distribution from our numerical simulations.

6.2 Salt migration due to inclination

In the second example, we consider two-layer structure of a greater extension, so that there are enough rock salt in the bottom layer to develop multi-diapirs. The migration is initiated

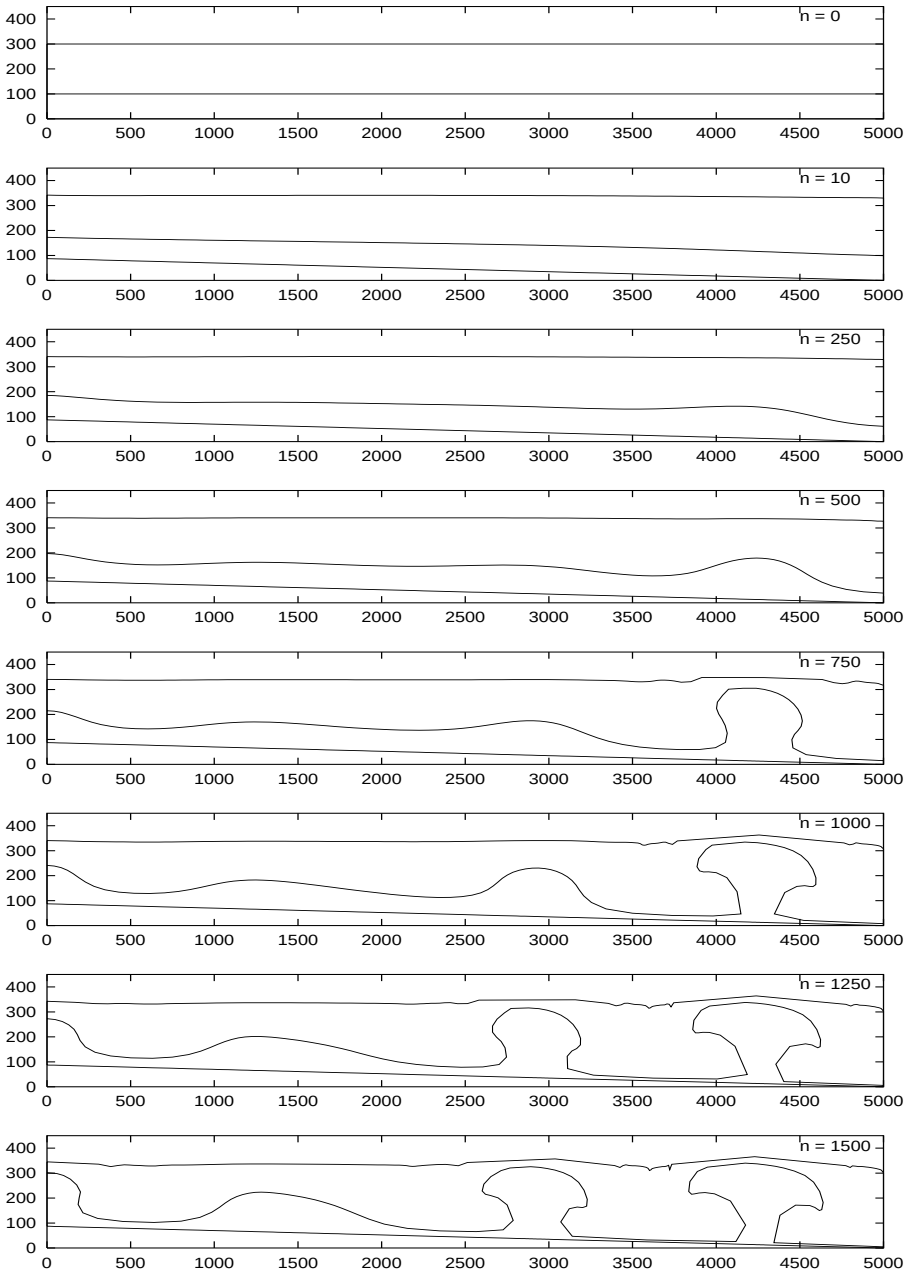

Figure 4: Salt migration initiated by a gradual lift of base rock to an angle of one degree at the initial 10 time steps on the left side. The figures show the growth sequence from right to the left for the appearance of salt structures.

by gradually lifting the base rock, which supports the salt layer, up to an inclination at an angle of one degree during the initial one million years ($n = 10$).

- The dimension of the initial state is: length = 5,000 m, height of salt layer = 100 m, height of sediment layer = 200 m. Initial rectangular mesh (100×30).
- The material parameters for rock salt are:
  $\rho_0 = 2.2\times10^3$ Kg/m^3, $s_1 = 0$, $s_2 = -0.2\times10^3$ Pa,
  $\lambda = -10.0\times10^3$ Pa Ma, $\mu_1 = 15.0\times10^3$ Pa Ma, $\mu_2 = \mu_3 = 0$, $\beta = 2\times10^9$ Pa.
- The material parameters for overburden sediment are:
  $\rho_0 = 3.0\times10^3$ Kg/m^3, $s_1 = 2.5\times10^3$ Pa, $s_2 = -7.5\times10^3$ Pa,
  $\lambda = \mu_1 = \mu_2 = \mu_3 = 0$, $\beta = 2\times10^9$ Pa.
- The incremental time: $\Delta t = 0.1$ Ma.

Due to the gravity, the lifting of the base rock on the left side pushes the body to the right which initiates the growth of a salt pillow at about the first 50 million years ($n = 500$) as can be seen from Fig. 4. As time goes on, an adjacent salt pillow appears as the first one becomes a salt diapir. The figures show the growth sequence from right to left of the appearance of different salt structures up to 150 million years ($n = 1500$).

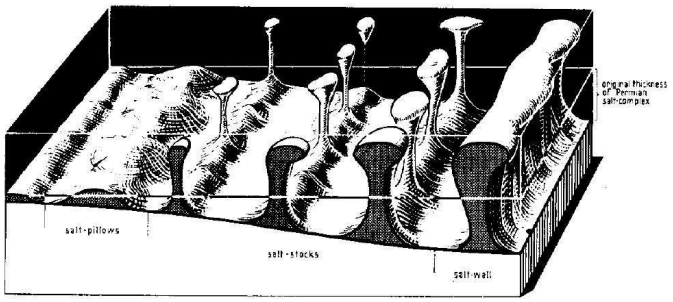

Figure 5: Diagram of different types of salt structure due to a dip at an angle of more than one degree in Northern Germany (From F. Trusheim, Bull. Amer. Assoc. Petroleum Geologists 44 (1960))

Such formation due to inclination of base rock was reported in permian salt complex of northern Germany as shown in the sketch (Fig. 5) by Trusheim [21]. Although our numerical simulation is only two-dimensional, the similarity of the formation of salt structure is rather striking. However, since the numerical data are of convenient choice only, the estimated time in million of years in numerical simulation may not be of any real significance.

7 Final remarks

The purpose of the present work is twofold. Firstly, we extend the successive linear approximation method proposed in [12, 10] for finite elasticity to viscoelasticity. This is indeed a straightforward extension except a few additional details. Secondly, numerical simulations for large deformation in sediment-salt migration are presented as an application of the SLA method.

The numerical capability of the SLA method has been verified by comparison with well-known universal solutions of finite elasticity in [12, 10]. With this confidence in mind, we apply this method to some problems in geomechanics of practical interest, which was the original motivation for this study in a research project. However, we do not attempt

quantitative validation of our simulations, because there are no geological field data nor comparable numerical results in the literature for consultation.

Remark 1: On material model

Although the problems of sediment-salt migration have been widely known and studied in salt tectonics and in petroleum industry. They usually were able to show some similar large deformation [13] by regarding the bodies as viscous fluids. However, from such results the stress distribution in the body would be of no meaningful physical significance because the body is a solid body instead. On the other hand, stress distribution from simulations (not shown in the paper) of our solid material models would be of real interest and render some useful information for petroleum industry.

Moreover, most of the material models used in those studies are rheological material models for fluid viscosity such as power law or something else [7, 8, 13]. In contrast, we have proposed solid material models based on the use of representation theorems for isotropic functions, which are well-known in constitutive theories of continuum mechanics. In fact, we are able to determine the material parameters, from uniaxial compression test for the sediment rock as Mooney–Rivlin material and uniaxial creep test for rock salt with the model (15), with very good agreement from experimental results of laboratory reports. However, for industrial research concerns, we do not show the numerical results with real material data. Instead, the numerical data for the simulations shown in this paper have been conveniently chosen. Nevertheless, we have found that the results of simulations with real material data are qualitatively equivalent to the ones presented in this paper.

Remark 2: On other incremental methods

For large deformations in finite elasticity, some incremental methods are widely known, for example, in the books by Ciarlet [2], Oden [15], and Ogden [16]. The methods usually concern small increments between successive boundary value problems formulated in the same domain of the *initial* reference configuration, i.e., in (total) Lagrangian formulation. This is the essential difference from the method proposed in this paper with the "updated" Lagrangian formulation, namely, the reference configuration is updated to the present state at each step. However, we refrain from calling the proposed method an *Updated Lagrangian formulation* (UL), because UL formulation is widely known in numerical literature (see for example [1]), for which the weak form of the problem is formulated in the Eulerian spatial domain, while the variable functions are expressed in the Lagrangian coordinate of the reference domain.

Remark 3: On small-on-large idea of linearization

For large deformations, systems of governing partial different equations are generally nonlinear. The boundary value problems are usually formulated in Lagrangian, arbitrary Lagrangian or Eulerian meshes, and numerical solution of nonlinear systems of discrete algebraic equations by Newton's type methods.

In this paper, we formulate boundary value problems in the coordinates relative to the configuration at the present time. In other words, we describe deformations relative to the present state, instead of a fixed (initial) reference configuration in the Lagrangian formulation. We call this the *Relative Lagrangian formulation* (it was called the *relative-descriptional formulation* in [10]).

The advantage of using the relative Lagrangian formulation is that we can consider a small time step from the present state, so that the constitutive function can be linearized relative to the present state, and the equation of motion becomes linear in relative displacement. When the present state proceeds in time, a nonlinear finite deformation can be treated as summation of successive small deformations in the same manner as the usual Euler's method

for solving differential equations, i.e., successively at each state, the tangent is calculated and used to extrapolate the neighboring state.

The essential idea of the proposed method is based on the approach of small deformation superposed on large deformation [5]. Although the *small-on-large* idea is very well-known, to our knowledge, numerical implementations of Euler's type successive approximation based on this idea have not been explored.

On the other hand, computational literature based on the *small-on-large* idea, typically the methods introduced in [17, 18, 22] are very well documented. Such methods, in which the nonlinear algebraic systems resulting from the variational formulation of the *nonlinear* boundary value problem are solved by Newton's method, employ the tangent operator obtained from small-on-large linearization of the constitutive functions and boundary conditions. Such methods are quite different from the one proposed in this paper concerning the use of the small-on-large approach. On the other hand, determination of tangent modulus, or equivalently the elasticity tensor, for material models is frequently discussed [14]. In the present paper, as an example, we consider a material model of Mooney–Rivlin type viscoelastic bodies and their elasticity and viscosity tensors are explicitly determined in the linearization.

In [19], the small-on-large idea is used in the formulation of elastodynamics, in the case of motions that have small displacement gradients with respect to a configuration that is a rigid motion from a fixed reference configuration, termed *small on rigid*. The constitutive equation is linearized similar to the one treated in this paper. However, the initial boundary value problem is formulated in the fixed reference configuration, i.e., the total Lagrangian formulation is employed, different from the relative Lagrangian formulation employing the intermediate preceding configuration as reference in this paper.

Acknowledgement This work is supported by a research project from Petrobras/Brasil. The authors (ISL, MAR) also acknowledge the partial support from research fellowship of CNPq, Brazil.

References

[1] Belytschko, T.; Liu, W.K.; Moran, B.: Nonlinear Finite Elements for Continua and Structures, John Wiley & Sons: Chichester, (2000).

[2] Ciarlet, P.G.: *Mathematical Elasticity, Volume. 1: Three-Dimensional Elasticity.* North-Holland: Amsterdam, 1988.

[3] Cipolatti, R., Liu, I-S., Rincon, M.A.: Mathematical analysis of successive linear approximation for Mooney–Rivlin material model in finite elasticity, Arxiv preprint arXiv:1107.2705

[4] Dixon, J.M.: Finite strain and progressive deformation in models of diapiric structures, *Tectonophysics* **28**, 89-124 (1975).

[5] Green, A.E.; Rivlin R.S.; Shield, R.T.: General theory of small elastic deformations superposed on finite deformations. *Pro. Roy. Soc. London*, Ser. A, **211**, 128-154, (1952).

[6] Hutter, K.; Jöhnk, K.: *Continuum Methods of Physical Modeling: Continuum Mechanics, Dimensional Analysis, Turbulence*, Springer, 2004.

[7] Ismail-Zadeh, A.T.; Huppert, H.E.; Lister, J.R.: Gravitational and buckling instabilities of rheologically layered structure: implications for salt diapirism, *Geophys. J. Int.*, **148**, 288-302 (2002).

[8] van Keken, P.E.; Spiers, C.J.; van den Berg, A.P.; Muyzert, E.J.: The effective viscosity of rocksalt: implementation of steady-state creep laws in numerical models of salt diapirism, *Tectonophysics* **225**, 457-476 (1993).

[9] Liu, I-S.: *Continuum Mechanics*, Springer: Berlin Heidelberg, 2002.

[10] Liu, I-S.: Successive linear approximation for boundary value problems of nonlinear elasticity in relative-descriptional formulation, *Int. J. Eng Sci.* **49**, 635-645 (2011).

[11] Liu, I-S.: A note on the Mooney–Rivlin material model, *Continuum Mech. and Thermody.* (2011), doi:10.1007/s00161-011-0197-6.

[12] Liu, I-S.; Cipolatti, R.A.; Rincon, M.A.: Successive linear approximation for finite elasticity, *Computational and Applied Mathematics* **29**, 465-478, (2010).

[13] Massimi, P.; Quarteroni, A.; Saleri, F.E.; Scrofani, G.: Modeling of Salt Tectonics. Comput. Methods Appl. Mech. Eng. 197, 281-293 (2007).

[14] Nicholson, D.W.; Lin, B.: On the tangent modulus tensor in hyperelasticity, *Acta Mechanica* **131**, 121-132 (1998).

[15] Oden, J.T.: *Finte Elements of Nonlinear Continua*. McGraw-Hill: New York, 1972.

[16] Ogden, R.W.: *Non-Linear Elastic Deformations*, Ellis Horwood: New York, 1984.

[17] Simo, J.C.; Hughes, T.J.R.: *Computational Inelasticity*, Springer: 1998.

[18] Simo, J.C.; Taylor, R.L.: Quasi-incompressible finite elasticity in principal stretches, continuum basis and numerical algorithms. *Computer Methods in Applied Mechanics and Engineering* **85**, 273-310 (1991).

[19] Tortorelli, D.A.: A generalized formulation of elastodynamics: small on rigid, *J. Elast.* **105**, 349-363 (2011).

[20] Truesdell, C.; Noll, W.: *The Non-Linear Field Theories of Mechanics*, 3rd edition. Springer: Berlin, 2004.

[21] Trusheim, F.: Mechanism of salt migration in northern Germany, *Bull. Amer. Assoc. Petroleum Geologists* **44**, 1519-1540 (1960).

[22] Zienkiewicz, O.C.; Taylor, R.L.: *The Finite Element Method*, Vol. 2: *Solid Mechanics*, Butterworth-Heinemann: Oxford, 2000.